MATERIAL RELIABILITY STUDY OF HIGH-SPEED SMALL CRAFT UNDER WAVE LOAD

Amalia Ika Wulandari[1], Alamsyah[1], Suardi[1], Wira Setiawan[1], Muhammad Uswah Pawara[1], Andi Mursid Nugraha Arifuddin[1], Husein Syahab[1]

[1]Department of Naval Architecture, Institut Teknologi Kalimantan, Balikpapan, Indonesia

E-mail: amaliaikaw@lecturer.itk.ac.id

Received: April 26, 2025 | **Accepted:** June 25, 2025 | **Published:** July 18, 2025

DOI: 10.12962/j27745449.v3i3.3921 | **Issue:** Volume 5 Number 3 2024 | **E-ISSN:** 2774-5449

ABSTRACT

This study focuses on analyzing the structural characteristics of a small craft constructed using aluminum alloy compared with sandwich material structure. High speed vessels are designed to address key performance challenges such as vessel motion, engine efficiency, fuel consumption, and cargo capacity. However, to endure extreme wave induced loads, enhancement of vessel's the structural strength is essential, especially in critical areas like the midship section. Analytical models and probabilistic methods are employed to predict structural performance under both constant and random wave loading conditions. Aluminum alloys are commonly chosen for fast boat construction due to their high strength to weight ratio and corrosion resistance. To evaluate structural behavior, simulations are carried out under varying wave heights and directions, providing insight into how the vessel performs in challenging marine environments. Load analysis is conducted using diffraction theory and the JONSWAP spectrum equation to determine the maximum bending moments experienced by the hull. The results show that both aluminum and sandwich structures exhibit similar reliability thresholds under wave-induced loading, but the sandwich structure consistently performs slightly better, with approximately 0.10% higher reliability. This suggests that sandwich materials offer improved structural integrity, making them the more suitable choice for high-speed small craft operating in wave conditions up to 2 meters. This analysis contributes to a deeper understanding of the reliability and performance of these materials, offering valuable guidance for designing and constructing high Small Crafts that perform efficiently and safely in demanding maritime operations.

Keyword: JONSWAP, Reliability, Ship Structure, Wave Load

Introduction

Maritime operations in certain regions necessitate the deployment of high-speed vessels, particularly small crafts, which are specifically designed to perform rapid tasks along coastlines [1]. These vessels are engineered to address four critical aspects of marine performance: vessel motion, engine capability, fuel consumption, and cargo capacity [2]. To meet these challenges, high-speed small crafts must possess not only agile maneuverability but also structural robustness capable of withstanding harsh ocean environments.

Due to the demanding nature of high-speed operations, the structural strength of these vessels must be enhanced to endure extreme wave induced loads that can compromise overall integrity [3]. A vessel in open water typically experiences six degrees of freedom (DOF) in motion: surge, sway, heave, roll, pitch, and yaw. These dynamic responses are primarily driven by wave loading on the vessel's hull and neglecting these effects may result in structural fatigue or even catastrophic failure.

Accordingly, the structural design and construction phases must place particular emphasis on strengthening critical regions of the hull especially the midship section where bending moments and structural stresses tend to concentrate [4]. To address these concerns, both deterministic and probabilistic analytical models are employed. Deterministic approaches assess structural integrity under assumed constant load conditions, while probabilistic models incorporate the random nature of sea states and wave induced bending moments.

The goal of structural reliability analysis in vessel design is to evaluate the safety margin between external wave induced loads and the internal structural resistance, especially under ultimate limit state (ULS) conditions. These include potential failure mechanisms such as local buckling and plastic yielding of materials [5]. To predict vessel motions and load distributions, numerical techniques such as linear potential flow theory (diffraction theory) are often employed [3]. Establishing boundary conditions for maximum loads typically involves adherence to classification society rules, physical material testing, and simulation-based approaches such as Finite Element Analysis (FEA) [6].

In terms of construction materials, modern fast boats frequently utilize lightweight alternatives such as aluminum alloys, carbon fiber reinforced plastic (CFRP), and high-density polyethylene (HDPE). Among aluminum alloys, series 5083 and 6061 are particularly popular in marine applications. While 5083 offers superior strength properties, 6061 is widely used due to its good corrosion resistance and formability [7].

Several prior studies have advanced the understanding of ship structural reliability. The work by Adiputra et al. [8] focused on reliability-based assessment at the girder level using finite element and empirical approaches. While informative regarding structural collapse modes, the study was confined to hull girder analysis and excluded hydrodynamic simulations, irregular wave effects, and directional wave loading. In contrast, more comprehensive reliability insights can be gained by incorporating hydrodynamic simulations based on irregular wave conditions and varying headings. Hafiz & Sulisetyono [4] analyzed the structural reliability of high-speed vessels constructed from CFRP materials to find out the most reliable structure design focusing on their research object. Although a reliable design was identified, the study did not incorporate material comparisons and limiting the generalizability of the conclusions. A broader understanding can be obtained through direct comparisons between different materials application under identical hydrodynamic loading. Sujiatanti et al. [9] conducted a reliability analysis considering hogging and sagging loads using FEM and Monte Carlo simulations. However, the absence of hydrodynamic modeling and irregular wave effects constrained the applicability of the findings to real-sea scenarios. Including sea state variability and wave directionality would allow for a more realistic depiction of structural performance under operational conditions. Xiao et al. [10] emphasized local structural reliability by combining probabilistic simulations with experimental validation. While this approach is valuable for localized structural components, the lack of global hydrodynamic response modeling and whole-structure analysis limits its relevance to full-ship performance evaluation. By addressing these gaps, a more robust structural reliability framework can be established for high-speed craft, particularly when assessing different material configurations under realistic marine environments.

The primary objective of this study is to evaluate the structural behavior of small crafts constructed using aluminum alloy 6061 under various wave induced loading conditions. Special attention is given to assessing the response of the hull under maximum bending moments across varying wave heights and headings. In addition, a comparative reliability analysis is performed between conventional aluminum structures and innovative sandwich material structures such as those with polyurethane core or foam core composites. The methodology involves developing a full-scale ship model to assess global bending loads induced by waves. Hydrodynamic simulations are carried out using a Boundary Element Method (BEM) based seakeeping analysis to estimate wave induced bending moments across different operating conditions. These loads are then compared against the ultimate strength capacities of the materials derived from aluminum and sandwich composite testing data to evaluate structural safety margins.

This comparison aims to identify the strengths and limitations of each material system in terms of structural reliability, fatigue performance, and damage tolerance. By integrating reliability-based design and material selection, this study seeks to contribute insights toward optimizing fast boat construction for challenging maritime environments. Such insights are crucial for informing future designs, particularly for operations in coastal security, patrol missions, rescue operations, and high-speed transport where performance and structural safety are paramount.

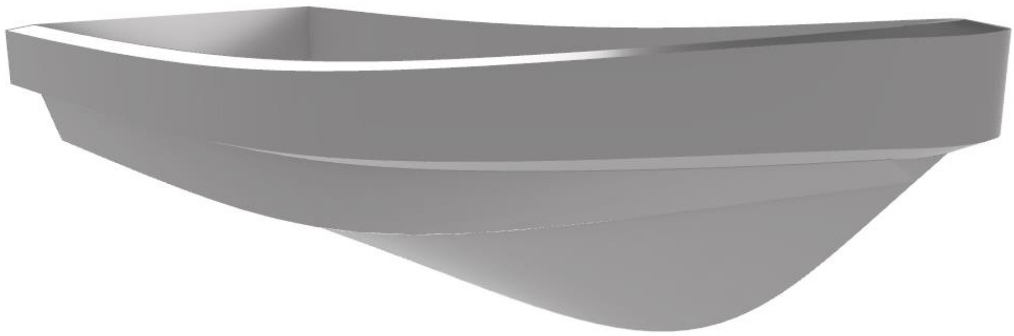

Figure 1. Small Craft hull perspective view

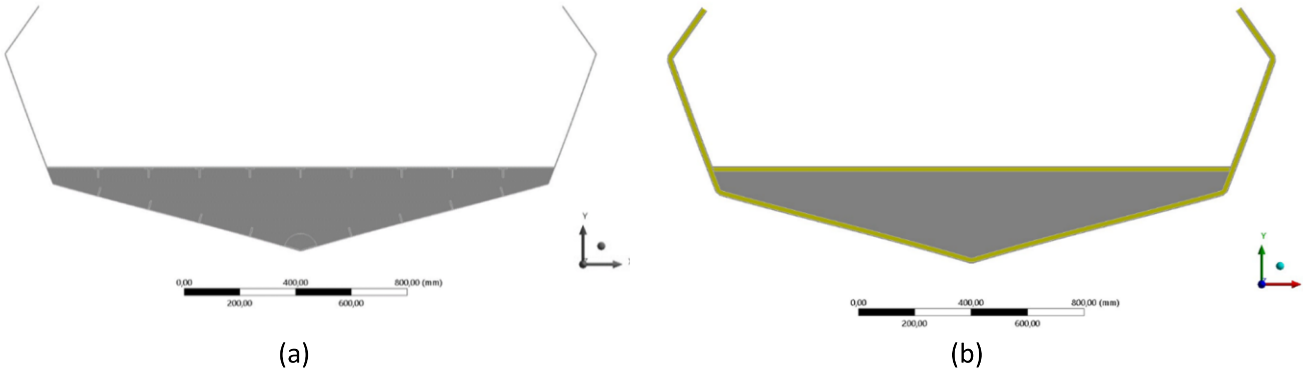

Figure 2. Ship midship Construction; (a) Aluminum. (b) Sandwich with Polyurethane Elastomer Core

Methodology

Small Craft Constructions and Materials

Ship structures play a critical role in maritime transportation by ensuring vessel safety, performance, and long-term durability [11]. In the context of shipbuilding especially for high performance small craft two widely adopted structural material systems are aluminum and sandwich composites. Each offers distinct advantages that cater to the specific demands of lightweight, high speed marine applications.

Aluminum is highly regarded for its excellent strength to weight ratio, corrosion resistance, and ease of fabrication, making it a preferred choice in small craft construction [12]. Marine grade aluminum alloys such as 5083 and 6061 are commonly employed due to their favourable mechanical properties and weldability. These characteristics are particularly advantageous in scenarios where weight reduction is essential without compromising structural integrity.

Conversely, sandwich composite structures typically comprising a lightweight core (e.g., polyurethane foam, honeycomb, or polymer foam) encased between two strong outer skins (such as fiberglass or carbon fiber laminates) provide remarkable benefits in terms of overall weight reduction, structural efficiency, and impact resistance [13,14]. These materials are especially attractive for small craft operating at high speeds, where minimizing mass while maintaining strength is essential for optimizing performance and fuel efficiency. The dimensions small craft analyzed in this study are shown in Table 1. The hull form is visualized in Figure 1.

Table 1. Small craft principal dimensions

Dimension	Size	Unit
Length	6.041	m
Breadth	2.432	m
Depth	1.795	m

The materials selected for this study are detailed in Table 2 and Table 3, highlighting key mechanical properties used in evaluating structural performance under marine loading conditions.

The midship construction of the small craft for each material visualized in Figure 2.

Table 2. Aluminum Material Properties

Properties	Magnitude	Unit
Density	2700	Kg/m^3
Young's Modulus	68900	MPa
Ultimate Tensile Strength	165	MPa
Poisson's Ratio	0.33	

Table 3. Polyurethane Elastomer Material Properties

Properties	Magnitude	Unit
Density	1124	Kg/m^3
Young's Modulus	181	MPa
Ultimate Tensile Strength	25	MPa
Poisson's Ratio	0.36	

Aluminum commonly used in small craft construction. This is because its favorable mechanical efficiency, resistance to marine corrosion, and manufacturability [15].

In this study, aluminum 6061 is employed for the hull structure. The main structural components include the deck, side plates, and bottom plates all with a thickness of 4 mm to ensure structural integrity without compromising weight. Additional reinforcements consist of T profiles (30 mm width × 50 mm height), transverse frames (4 mm thickness), flat bars (50 mm width × 5 mm thickness), and angle keelsons (60 mm width × 6 mm thickness), which collectively enhance the hull's rigidity and resistance to dynamic loads during operation. Sandwich structures are increasingly used in ship construction, particularly in scenarios where weight reduction is a critical design consideration. These structures are composed of a lightweight core material sandwiched between two outer layers, offering numerous advantages such as reduced overall weight, enhanced strength and stiffness, improved load distribution, as well as beneficial sound and thermal insulation properties. The calculation of sandwich material thickness can be approached using Eq. (1)-(3).

$$R = 0.01\, A_R 0.1 \left[\frac{b^2}{d(t_1+t_2} + 11.7\left(\frac{bt_c}{d^2}\right)^{1,3}\right] \quad (1)$$

$$A_R = \left(\frac{a}{b}\right)^{0.65} \quad (2)$$

$$P_{eq.R} = 0.0017 \quad (3)$$

Their inherent design flexibility also makes them highly suitable for a wide range of shipbuilding applications [16–19]. In comparison with traditional aluminum hull designs, the sandwich structure eliminates the need for longitudinal profiles, as the core material itself provides the required strength. This substitution demonstrates the efficiency of the sandwich structure in maintaining structural integrity while reducing weight. To determine the appropriate thickness of the sandwich material, a specific calculation approach is employed, which considers the panel dimensions, material properties, and stiffener spacing [20]. Based on the calculation, the sandwich structure adopted in this study consists of 4 mm thick alumunium face plates (top and bottom) and a 15 mm thick core with the design as shown in Figure 3.

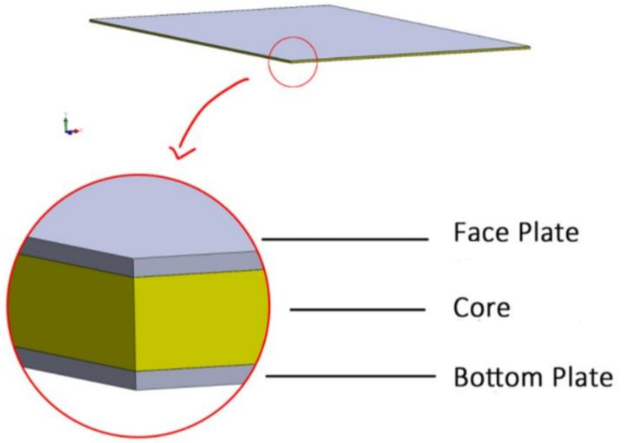

Figure 3. Sandwich configuration illustration

Operational Condition

The operational area of the small craft selected for analysis will be simulated under a range of wave conditions. The significant wave heights considered in the simulation are shown in Table 4. This height was taken as parameter to analyze the structure condition upon variation of heights that could be encountered in the operational area [21]. In addition, wave heading directions of 0° (Following sea), 90° (beam sea), and 180° (head sea) are included, which illustrated in Figure 4.

Following the predetermined variations in wave height, a load analysis was carried out to determine the maximum bending moment values. This analysis utilizes diffraction theory (see Eq. (4)) to model wave–structure interactions and applies the JONSWAP spectrum to represent the energy distribution of an irregular sea state [22, 23].

$$S(\omega) = \frac{ag^2}{\omega^5} exp\left[-\beta\,\frac{\omega^4 p}{\omega^4}\right]\gamma^{\alpha} \quad (4)$$

A JONSWAP based hydrodynamic diffraction analysis was then performed, and the resulting data can be seen in Figure 5.

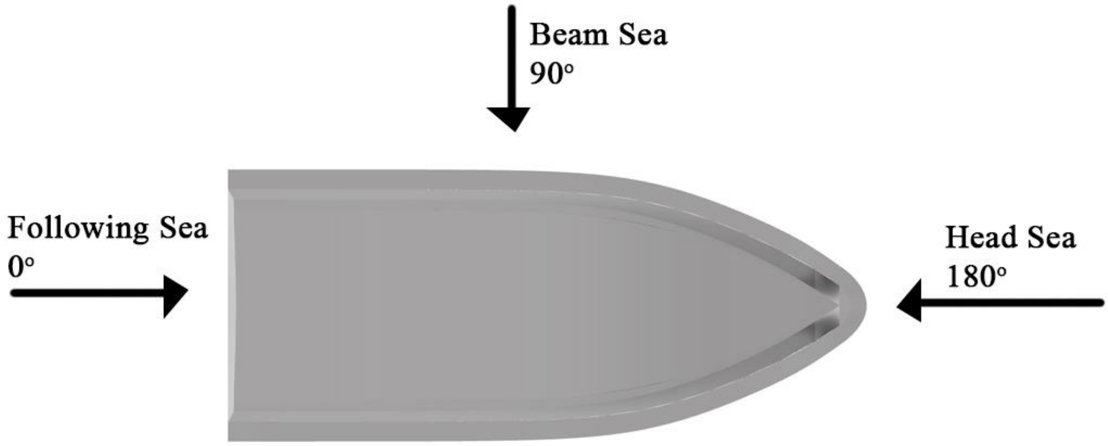

Figure 4. Wave heading direction

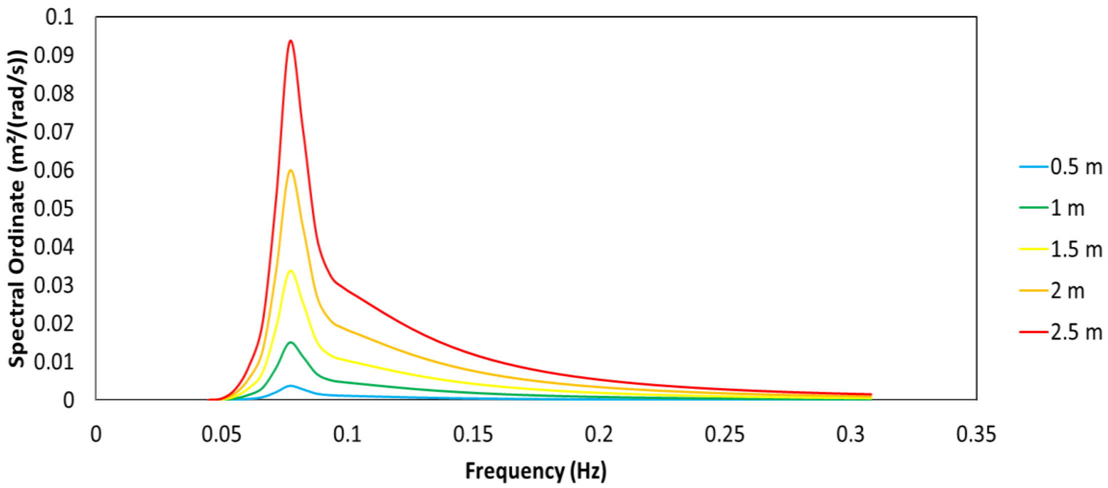

Figure 5. JONSWAP Wave Spectrum

Table 4. Significant wave height for the analysis

Wave Height (m)
0.5
1
1.5
2
2.5

Load Calculation

The analysis in this study focused on obtaining the maximum bending moment values through simulation. Shear force and bending moment distributions along a structure are calculated with respect to a specified neutral axis, which can be aligned with one of the global reference axes either X, Y, or Z. These calculations are made while the structure is in equilibrium, and they are essential for understanding how external and internal loads affect the structural behavior under wave conditions [24].

For instance, consider the case where the distribution of shear force and bending moment is needed along a neutral axis that runs parallel to the fixed reference X-axis, with the structure in its equilibrium state. In this setup, the coordinate system NXYZ is established, in which the X-axis serves as the neutral axis, while the Y- and Z-axes align with the corresponding fixed reference axes. The mass is distributed from the stern to the bow, and for any cross-section perpendicular to the neutral axis, its intersection with the axis is defined at a specific position within the NXYZ frame.

Then, the external hydrodynamic moment can be assumed using Eq. (5).

$$M_f(\omega, x_0) = \iint_{S_x} [(x - x_0) \times (-pn)] dS \tag{5}$$

In this context, ω\omega represents the wave frequency, Sx denotes the portion of the wetted surface extending from the stern to the specified cross-section, and P refers to the combined hydrostatic and total hydrodynamic pressures, which include contributions from the incident wave, diffraction wave, radiation wave, and variations in hydrostatic pressure. The vector n indicates the normal to the wetted hull surface, oriented outward toward the fluid domain. The bending moment is calculated with respect to the intersection point X0. If the linearized drag effects relative to the intersection point X0 on tube and disc elements (commonly found in ship hull form) are considered, they can be determined using Eq. (6)

$$r_t = X_{t-}X_O = (x_t, y_t, z_t) \tag{6}$$

The contribution of the linearized drag effect to the resulting distribution at the intersection point X0 is calculated by summing the influence across all tube and disc elements that fall within the range of [Xs, X0].

Gravitational effects at the same intersection point X0 are quantified based on Eq. (7):

$$M_f(\omega,,x) = \sum_{x=x_s}^{x}\{(X_j - X_0\} \times \left[(0,0,-m_j g) - \theta \times (0,0,-m_j g)\right] \tag{7}$$

In this context, θ = (θ1, θ2, θ3) represents the rotational response, while mj and Xj denote the mass and geometric center between the limits [Xs, X0]. Inertia-related contributions to the overall response with respect to point X0 are given in Eq. (8).

$$M_m(\omega,,x) = \sum_{x=x_s}^{x_0}\{m_j(X_j - X_0\} \times (u_j, v_j, w_j) + (\theta_1, \theta_2, \theta_3)\left[I_{xxj}\right] \tag{8}$$

Here, (u_j,v_j,w_j) describes the translational motion of the center of mass for the $j_{\text{-th}}$ segment, and $[I_{xx}]$ corresponds to the moment of inertia matrix associated with the same segment. The total static contribution, comprising only hydrostatic and gravitational effects, is identified as the hydrostatic shear force and bending moment. These are derived by summing the relevant static components from the governing relations. In contrast, all other associated terms constitute the dynamic shear force and bending moment. To identify the critical response at a given location, the peak amplitude of the bending moment (M_B) response across the full range of wave frequencies is used. This peak value is referred to as the shear force or bending moment envelope for that section. When evaluating these distributions along a neutral axis aligned with either the fixed reference Y- or Z-axis, the same principles of integration and summation apply, but are executed along the corresponding axis direction [24]. In this simulation, the gamma value for irregular wave assumption was set to the default of 3.3, while the peak frequency was defined as 0.48 rad/s. Simulations were carried out using hydrodynamic diffraction analysis over a duration of 20 seconds with a time step of 0.001 seconds, resulting in a total of 10,001 computational steps for each variation. The maximum stress value (σ) generally occurs in the midship section and is calculated by multiplying the bending moment (M_B) with the centroid (Z_B), then dividing by the moment of inertia of the midship section (I_{yB}) [4], which can be seen in Eq. (9).

$$\sigma = \frac{M_B \, x \, Z_B}{I_{yB}} \tag{9}$$

The structural analysis of the Small Craft also incorporates the Weibull distribution equation, which is widely used in reliability and failure rate analysis. This distribution effectively represents the probability of structural failure and helps in evaluating the structural reliability of the vessel. The results of the Weibull distribution yield a bell shaped curve. The input data for this analysis include load distribution values obtained from simulation and strength distribution values derived from finite element analysis (FEA) of the midship section, as this area experiences the highest bending moment [25]. The normal distribution equation used in this context shown in Eq. (10).

$$f(x) = \frac{1}{\sigma\sqrt{2\pi}} e^{-\frac{1}{2}(\frac{x-\mu}{\sigma})^2} \tag{10}$$

Hydrodynamic Analysis

This study utilizes two complementary numerical approaches to analyze the hydrodynamic behavior and structural response of small craft hulls subjected to wave action: a finite element model (FEM) and a boundary element method (BEM) based hydrodynamic model. The BEM model, formulated under potential flow theory, enables efficient computation of motion responses and hydrodynamic forces. While FEM solves partial differential equations over the entire structural domain, BEM transforms these into boundary integrals, significantly reducing the problem's dimensionality. This reduction is particularly advantageous in wave structure interaction problems, where only the wetted surface of the hull is considered, simplifying the meshing process and making it well suited for modeling infinite fluid domains such as open seas [26]. The motion of the small craft is governed by the interaction between the incident waves and the submerged geometry of the hull. During waves induced oscillation, variations in wetted surface area alter the pressure distribution along the hull, influencing both motion characteristics and internal structural loads. For the fluid domain, the governing assumptions include inviscid, incompressible, and irrotational flow, which leads to the formulation of the Laplace equation for the velocity potential ϕ as seen in Eq. (11).

$$\nabla^2 \phi = 0 \tag{11}$$

In Cartesian coordinates (x,y,z), this expands to Eq. (12):

$$\frac{\partial^2 \phi}{\partial x^2} + \frac{\partial^2 \phi}{\partial y^2} + \frac{\partial^2 \phi}{\partial z^2} \tag{12}$$

The appropriate boundary conditions are applied at the free surface, hull boundary, and seabed. For example, at the seabed, a no flux condition is enforced as in Eq. (13)

$$\frac{\partial \phi}{\partial z} = 0 \tag{13}$$

The analysis configuration is shown in Figure 6(a) and wave simulation are illustrated in Figure 6(b). The computational domain is defined with a total length of 10L and a width of 5L, where L represents the characteristic length of the model, typically the length of the vessel. This sizing ensures sufficient space is allocated for wave development and propagation during the simulation. The upstream boundary is positioned at a distance of 2L ahead of the fore perpendicular (FP), while the downstream boundary extends 7L beyond the aft perpendicular (AP), allowing the flow and wave patterns to evolve without artificial reflections or boundary interference.

Reliability Assessment

In this study, the structural reliability analysis was conducted by comparing the stress-based load distribution resulting from wave-induced bending moments with the corresponding material strength distribution. The approach follows a probabilistic framework commonly adopted in reliability engineering, as outlined by Ang and Tang [27]. First, stress values derived from the simulation results. These stress values were then statistically treated to form a probability density function (PDF), representing the distribution of applied loads on the structure. Concurrently, strength data were compiled from experimental studies on the materials used, which were then also transformed into a corresponding PDF to represent the structural resistance. By comparing these two distributions, the reliability of the structure was assessed. The overlapping area between the load and strength distributions represents the probability of failure, while the non-overlapping portion indicates the probability of the structure withstanding the applied stresses. The reliability value is thus determined as one minus the failure probability. To provide a more quantifiable measure of reliability, the safety factor (β) was calculated using the statistical properties of both distributions, obtained in Eq. (14)

$$\beta = \frac{\mu s - \mu z}{\sqrt{\sigma_s^2 + \sigma_z^2}} \tag{14}$$

In the context of structural reliability analysis, the parameter μ_s refers to the mean value of the material strength distribution, representing the typical or average strength that the structure's material can withstand. On the other hand, μ_z denotes the mean value of the load or stress distribution, indicating the average stress experienced by the structure under operating conditions. The term σ_s represents the standard deviation of the strength, which reflects the variability or uncertainty in the material's resistance capacity. Likewise, σ_z is the standard deviation of the applied stress or load, capturing the degree of fluctuation or inconsistency in the loading conditions.

Result and Discussion

Load and Strength Distribution

The load distribution graph presented in Figure 7 was derived from the bending moment results obtained through hydrodynamic simulations, which were conducted under five different wave heights and three wave directions, resulting in a total of 15 unique load cases.

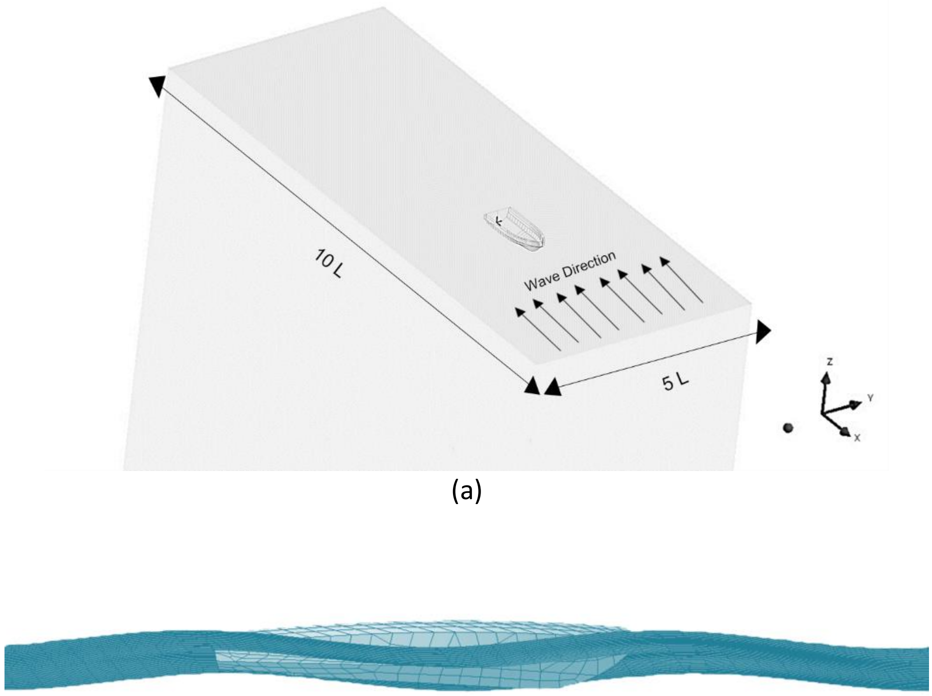

(a)

(b)

Figure 6. Hydrodynamic analysis configuration using Boundary Element Method (BEM); (a) Boundary condition, (b) Illustration of wave simulation along the hull.

Table 5. Load distribution data

Wave Heights (m)	Wave Heading (°)	Max Bending Moment (N.m)	Stress (MPa)
0.5	0	626700	41.27
0.5	90	674715	44.44
0.5	180	995619	65.57
1	0	1259970	82.98
1	90	815550	53.71
1	180	3265782	215.08
1.5	0	1928872	127.03
1.5	90	1169052	76.99
1.5	180	2942180	193.77
2	0	2613624	172.13
2	90	1657300	109.15
2	180	3921669	258.28
2.5	0	3319883	218.65
2.5	90	3862900	254.41
2.5	180	4946458	325.77
Inertia	**Zb**	**μz**	**σz**
1376983	90.688	149.28	91.124

Each of these bending moments values were then converted into corresponding stress values using Eq. (9), enabling a consistent basis for structural assessment. In this context, the resulting stress values are treated as the "load," since they directly reflect the structural demand induced by external hydrodynamic forces. The loads of each operational condition concluded in Table 5 and the comparison of each can be seen in Figure 8. These calculated loads were then compiled into a distribution curve comprising 1,000 interpolated data points to capture the variation and statistical behaviour of the loading conditions, illustrated in Figure 9. This load distribution was subsequently compared against the "strength" distribution, which was constructed from sampled data in material strength studies, allowing for reliability assessment based on the probability of failure due to stress exceeding material capacity. The strength data distribution process employed in this study specifically focuses on the ultimate tensile strength of the materials. This process involves collecting and analyzing data from previous research to gain a comprehensive understanding of the material's capacity to endure maximum tensile stress before failure. Such understanding is vital in the context of ship structure reliability analysis, as it supports the evaluation of structural performance and reliability under various operational conditions. The insights gained from this analysis contribute significantly to the design of safe and durable ship structures. The strength distribution data for aluminum materials [28–32] and sandwich structures [33–38], shown in Figure 10 and 11.

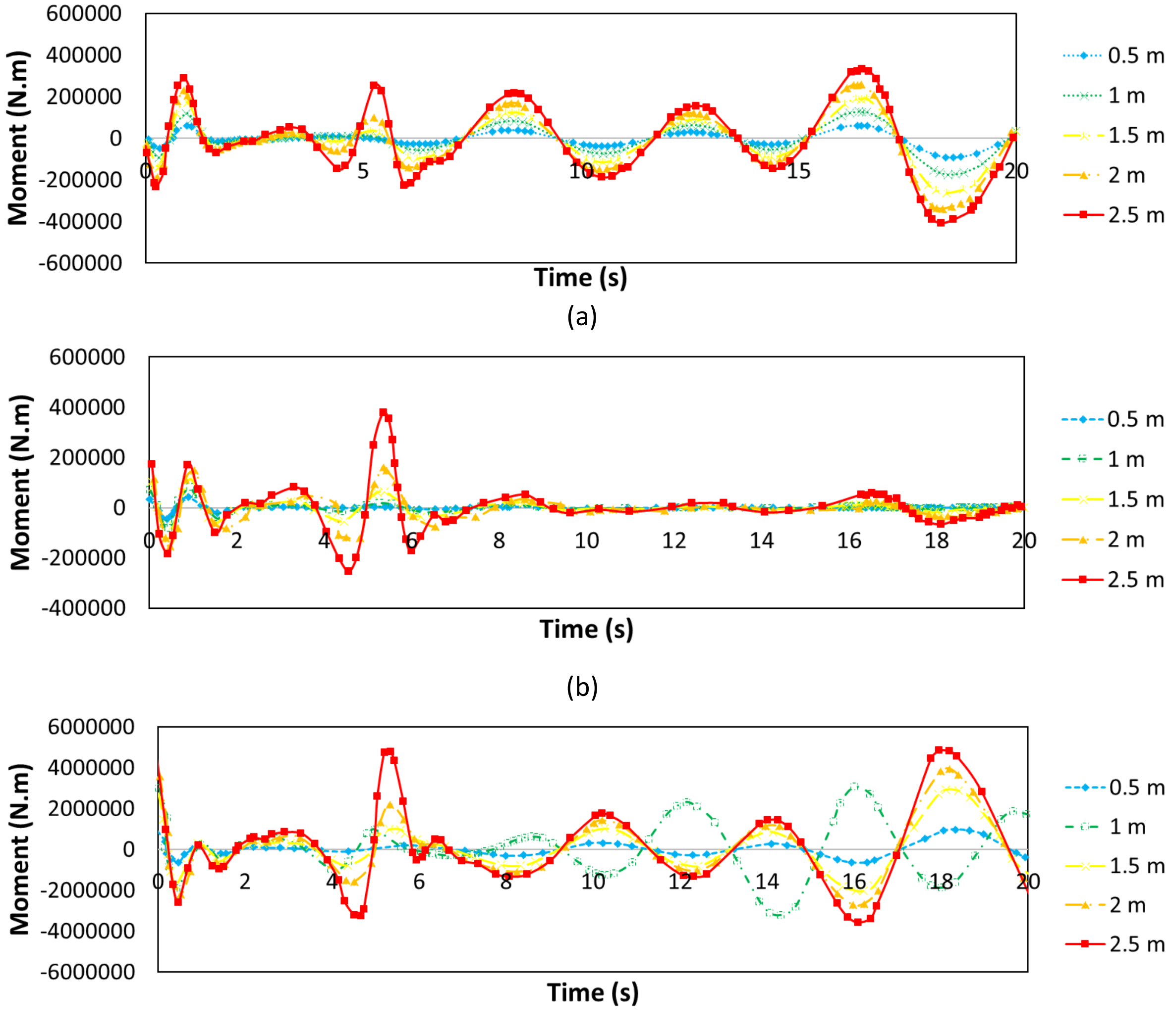

Figure 1. Bending moment comparison on every significant wave height; (a) Head Sea, (b) Beam Sea. (c) Following Sea.

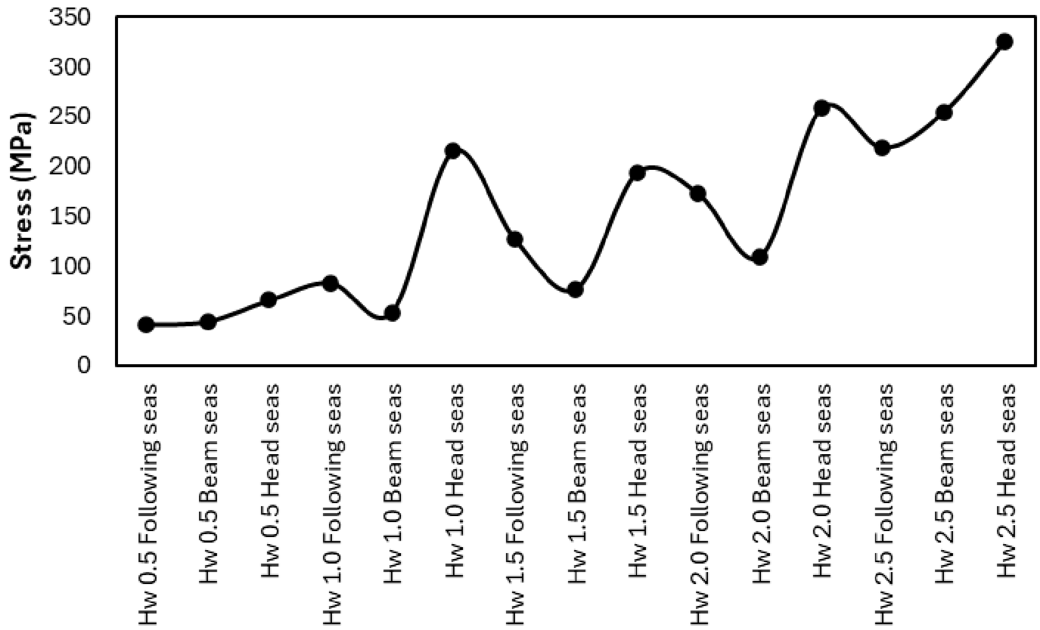

Figure 8. Load distribution between operational conditions

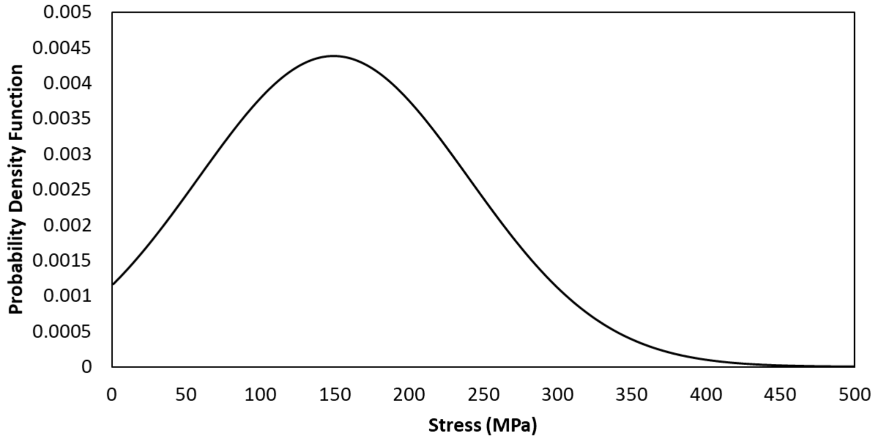

Figure 9. Load distribution graph

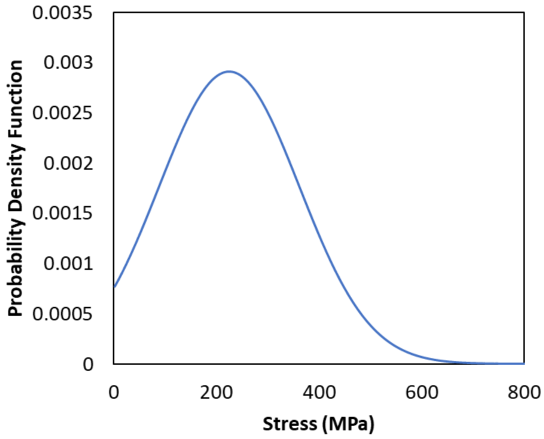

Figure 2. Strength distribution graph for aluminum structure

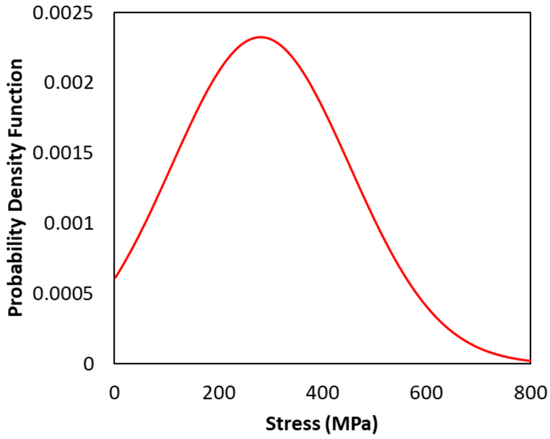

Figure 3. Strength distribution graph for sandwich structure

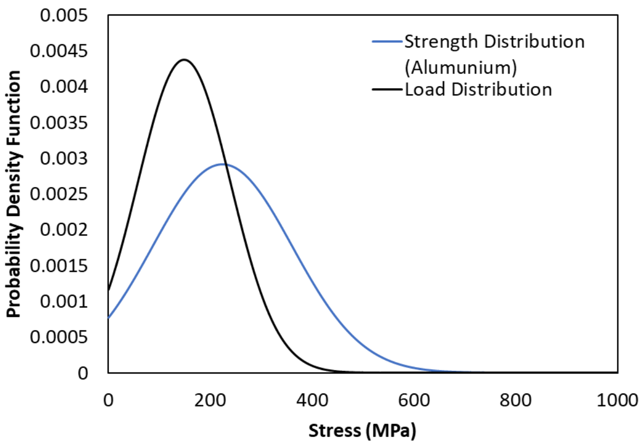

Figure 4. Comparison of Load against strength of Aluminum Structure

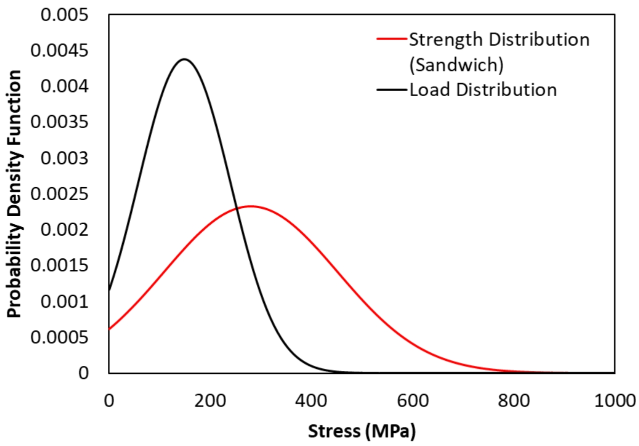

Figure 5. Comparison of Load against strength of Sandwich Structure

Reliability Analysis

The analysis process involves comparing the strength distribution obtained from finite element analysis with the load distribution to assess the structural reliability of the small craft. This comparison allows for evaluating whether the material and structural configuration can withstand the operational loads. The comparison between the materials' strength distribution with the overall corresponding load distribution is illustrated in Figure 12 for alumunium and Figure 13 for sandwich structure.

Table 1. Structure reliability on each wave height variations

Wave Height (m)	Alumunium			Sandwich		
	Failure	Reliability	β	Failure	Reliability	β
0.5–1	15.85%	84.15%	1.98	15.02%	84.98%	1.91
1–1.5	21.65%	78.35%	1.67	20.89%	79.11%	1.62
1.5–2	29.43%	70.57%	1.44	28.94%	71.06%	1.4
2–2.5	40.27%	59.73%	0.9	39.35%	60.65%	0.9
Total	34.54%	65.46%	1.35	34.44%	65.56%	1.33

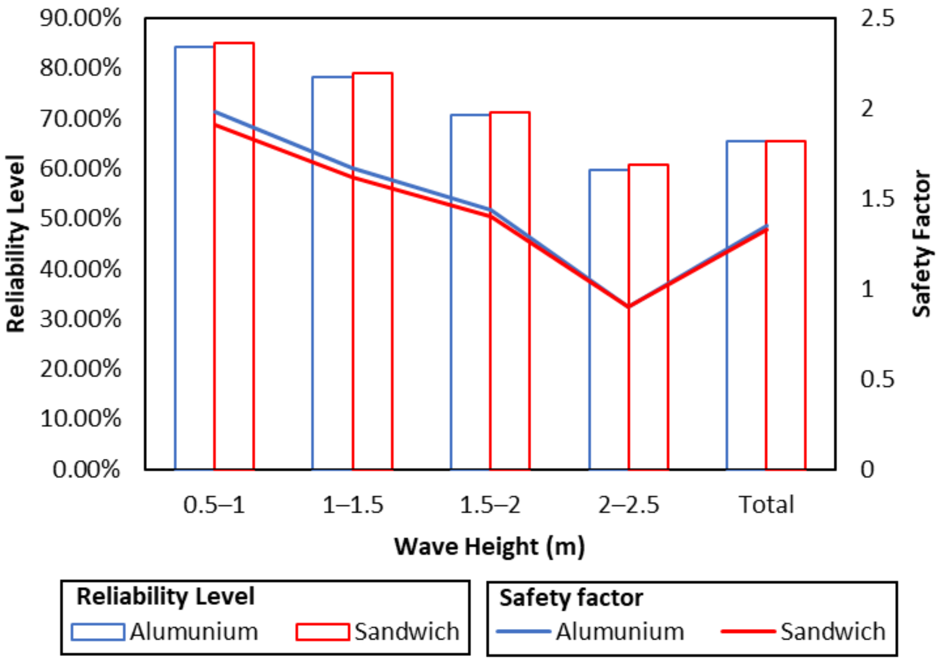

Figure 14. Structure reliability on each wave height variations

The load distribution curve illustrates the external forces acting on the Small Craft during operation, representing the magnitude and distribution of the applied loads. In contrast, the strength distribution curve reflects the structural strength derived from finite element analysis, indicating the structure's ability to resist those loads. The intersecting area between the load and strength distribution curves is a key indicator of structural reliability. A larger intersecting area signifies a higher level of reliability, as it implies that the structure's strength consistently meets or exceeds the applied loads under various operating conditions. This suggests the structure can withstand forces without experiencing excessive stress or failure.

Table 6 and Figure 14 present the reliability analysis results under varying wave heights. As shown, the aluminum structure has a total failure probability of 34.54%, corresponding to a reliability level of 65.46%. In comparison, the sandwich structure shows a slightly lower failure probability of 34.44% and a reliability of 65.56%, indicating marginally better performance in resisting structural failure. At the lowest wave range (0.5–1 m), the sandwich structure shows a failure probability of 15.02%, slightly lower than the aluminum structure's 15.85%. This trend continues across all wave heights, with the sandwich structure consistently exhibiting a lower probability of failure. At the most critical condition (2–2.5 m wave height), the sandwich structure shows a failure probability of 39.35%, compared to 40.27% for aluminum. These results suggest that the sandwich material maintains better performance under increasing wave loads. Based on these findings, the recommended maximum operational condition for both structures is around a 2-meter wave height, beyond which reliability decreases significantly.

Conclusion

This study aimed to evaluate the structural reliability of aluminum and sandwich composite materials for application in Small Craft construction, particularly under varying wave load conditions. The primary objective was to compare the capacity of both materials to withstand operational stress and to identify which offers better reliability for marine environments. The methodology involved conducting hydrodynamic simulations to obtain bending moment values across different wave heights and directions. These bending moments were then converted into stress values, which were interpreted as load distributions. The load data were compared against material strength distributions collected from literature, and a reliability index was calculated using statistical analysis. This approach allowed for a probabilistic assessment of each material's performance under realistic loading scenarios. A comprehensive assessment of the reliability levels for aluminum and sandwich structures was conducted based on their respective material properties. Aluminum is widely recognized for its high strength-to-weight ratio, making it a preferred material in shipbuilding. In contrast, the sandwich structure, comprising a lightweight core between two outer layers, offers additional advantages such as reduced weight, enhanced stiffness, improved load distribution, sustainability, and greater design flexibility. The comparative analysis revealed that the sandwich structure demonstrates a slightly higher reliability level—approximately 0.10% greater than that of aluminum. This suggests that the sandwich structure has a better capacity to withstand applied loads, offering improved structural integrity and reliability. Although both materials exhibit similar reliability thresholds, the sandwich structure consistently performs better across varying wave conditions. It can therefore be inferred that the safest maximum operational wave height for both structures is approximately 2 meters. Based on the reliability assessment and intersecting area analysis, the sandwich structure is recommended as the more suitable material for high-performance Small Craft construction. Its superior performance in resisting failure under demanding marine conditions supports its use for ensuring vessel safety, durability, and operational efficiency.

References

[1] E.S. Hadi, S. Jokosisworo, and Widyanto, Analisa performa hullform pada pra perancangan speed boat katamaran untuk search and rescue (SAR) di Pantai Gunungkidul Yogyakarta berbasis CFD, KAPAL 9 (2012).

[2] O.M. Faltinsen, Hydrodynamics of High-Speed Marine Vehicles, Cambridge University Press, 2006.

[3] A. Sulisetyono and M. Kadhafi, Fatigue life prediction for warship operation in Indonesian water, Applied Mechanics and Materials 874 (2018) 140–146. DOI: 10.4028/www.scientific.net/AMM.874.140.

[4] [M.A. Hafiz and A. Sulisetyono, Structural reliability analysis for the construction design of the high-speed ship with CFRP material, IOP Conf Ser Earth Environ Sci 1081 (2022) 012041.

[5] Harrison, An introduction to structural computation, in: Structural Analysis and Design, Elsevier, 1990, pp. 1–9.

[6] S. Ekşı and K. Genel, Comparison of mechanical properties of unidirectional and woven carbon, glass and aramid fiber reinforced epoxy composites, Acta Phys Pol A 132 (2017) 879–882.

[7] M.A. Rizki, Analisis pengaruh variasi elektroda pada pengelasan aluminum 5083 dengan 6061 terhadap sifat mekanik, struktur mikro, dan prediksi korosi, Teknik ITS (2018).

[8] [R. Adiputra, T. Yoshikawa, and E. Erwandi, Reliability-based assessment of ship hull girder ultimate strength, Curved and Layered Structures 10 (2023). DOI: 10.1515/cls-2022-0189.

[9] S.H. Sujiatanti, A. Baihaqi, A. Sulisetyono, R. Pujiwat, S. Rahmadianto, and R. Ramli, Safety and reliability analysis of the ship structure due to sagging and hogging loads for infrastructure sustainability, IOP Conf Ser Earth Environ Sci 1461 (2025) 012012.

[10] S. Xiao, Y. Han, Y. Zhang, Q. Wei, Y. Wang, N. Wang, H. Wang, J. Liu, and Y. Liu, A reliability analysis framework of ship local structure based on efficient probabilistic simulation and experimental data fusion, Metals (Basel) 12 (2022) 805. DOI: 10.3390/met12050805.

[11] O.F. Hughes and J.K. Paik, Ship Structural Analysis and Design, Society of Naval Architects and Marine Engineers, New Jersey, 2010.

[12] M.A. Wahid, A.N. Siddiquee, and Z.A. Khan, Aluminum alloys in marine construction: characteristics, application, and problems from a

fabrication viewpoint, Marine Systems & Ocean Technology 15 (2020) 70–80.
[13] K.V. Ramakrishnan and P.G. Kumar, Applications of sandwich plate system for ship structures, Journal of Mechanical and Civil Engineering (2016) 83–90.
[14] A. Zubaydi and A. Budipriyanto, Sandwich Material: Theory, Design, and Application, Airlangga University Press, Surabaya, 2020.
[15] [15] Riswanda, Akhyar, Sugianto, H. Kadir, and S. Rizal, Numerical simulation of the effect of shoulder rotation on the tensile strength of FSW dissimilar joints of aluminum alloy, Defect and Diffusion Forum 402 (2020) 90–99.
R.C. Ariesta, A. Zubaydi, A. Ismail, and T. Tuswan, Damage evaluation of sandwich material on side plate hull using experimental modal analysis, Mater Today Proc 47 (2021) 2310–2314.
[16] H. Siswanti, A. Zubaydi, B. Piscesa, H. Syahab, and R.C. Ariesta, Study of polyurethane elastomer cores interfacial fracture resistance of the sandwich materials for ship structures, IOP Conf Ser Earth Environ Sci 1461 (2025) 012005.
[17] A. Ismail, A. Zubaydi, B. Piscesa, R.C. Ariesta, and T. Tuswan, Vibration-based damage identification for ship sandwich plate using finite element method, Open Engineering 10 (2020) 744–752. DOI: 10.1515/eng-2020-0086.
[18] T. Tuswan, A. Zubaydi, B. Piscesa, A. Ismail, C. Rizky, F. Ilham, and I. Fikri, Influence of application of sandwich panel on static and dynamic behaviour of ferry ro-ro ramp door, Journal of Applied Engineering Science 19 (2021) 208–216. DOI: 10.5937/jaes0-27708.
[19] Lloyd Register, Rules for the Application of Sandwich Panel Construction to Ship Structure, 2022.
[21] BMKG, BMKG Ocean Forecast System, 2023.
[22] U.-J. Lee, W.-M. Jeong, and H.-Y. Cho, Estimation and analysis of JONSWAP spectrum parameter using observed data around Korean coast, J Mar Sci Eng 10 (2022) 578. DOI: 10.3390/jmse10050578.
[23] M.I. Jifaturrohman, I.K.A.P. Utama, T. Putranto, D. Setyawan, and L. Huang, A study into the correlation between single array-hull configurations and wave spectrum for floating solar photovoltaic systems, Ocean Engineering 312 (2024) 119312.
[24] ANSYS, AQWA User Manual, 2012.
[25] L.G. Otaya, Distribusi probabilitas Weibull dan aplikasinya, Jurnal Manajemen Pendidikan Islam (2016).
[26] R. Datta and C. Guedes Soares, Analysis of the hydroelastic effect on a container vessel using coupled BEM–FEM method in the time domain, Ships and Offshore Structures 15 (2020) 393–402. DOI: 10.1080/17445302.2019.1625848.
[27] A.H.S. Ang and W.H. Tang, Probability Concepts in Engineering, John Wiley & Sons, United States of America, 2007.
[28] Gabrian International, 6061 Aluminum: Get to Know its Properties and Uses.
[29] AZO Materials, Aluminum: Specifications, Properties, Classifications and Classes.
[30] ASM, Aluminum 6061-T6; 6061-T651.
[31] Ferguson Perforating, 6061 Aluminum Alloy.
[32] AmesWeb, Aluminum Alloys - Yield Strength and Tensile Strength.
[33] H. Alshahrani, A. Ahmed, H. Kabrein, and V.R.A. Prakash, Mechanical properties study on sandwich composites of glass fiber reinforced plastics (GFRP) using liquid thermoplastic resin, Elium®: Preliminary experiments, Coatings 12 (2022) 1423. DOI: 10.3390/coatings12101423.
[34] X. Zhao, L. Tan, and F. Zhang, Mechanical behavior of sandwich panels with hybrid PU foam core, Advances in Civil Engineering 2020 (2020) 1–8. DOI: 10.1155/2020/2908054.
[35] B.J. Kim, Study on applicability of ultimate strength design formula for sandwich panels – application cases of double hull tanker bottom structures, Journal of Ocean Engineering and Technology 34 (2020) 97–109.
[36] M.A. Azmi, H.Z. Abdullah, and M.I. Idris, Properties of polyurethane foam/coconut coir fiber as a core material and as a sandwich composites component, IOP Conf Ser Mater Sci Eng 50 (2013) 012067. DOI: 10.1088/1757-899X/50/1/012067.
[37] P. Arianto, A. Zubaydi, B. Piscesa, and T. Tuswan, Experimental and numerical bending analysis of steel/resin-talk sandwich material, IPTEK The Journal for Technology and Science 30 (2019) 123. DOI: 10.12962/j20882033.v30i3.5496.
[38] Total Materia, Sandwich Steel Panels: Part Two.